Supporting Information Appendix

The vitamin D receptor as a master regulator of the c-MYC/MXD1 network.

Reyhaneh Salehi-Tabar, Loan Nguyen-Yamamoto, Luz E. Tavera-Mendoza, Thomas Quail, Vassil Dimitrov, Beum-Soo An , Leon Glass, David Goltzman, and John H. White

Supplemental figures, Experimental Procedures, and tables

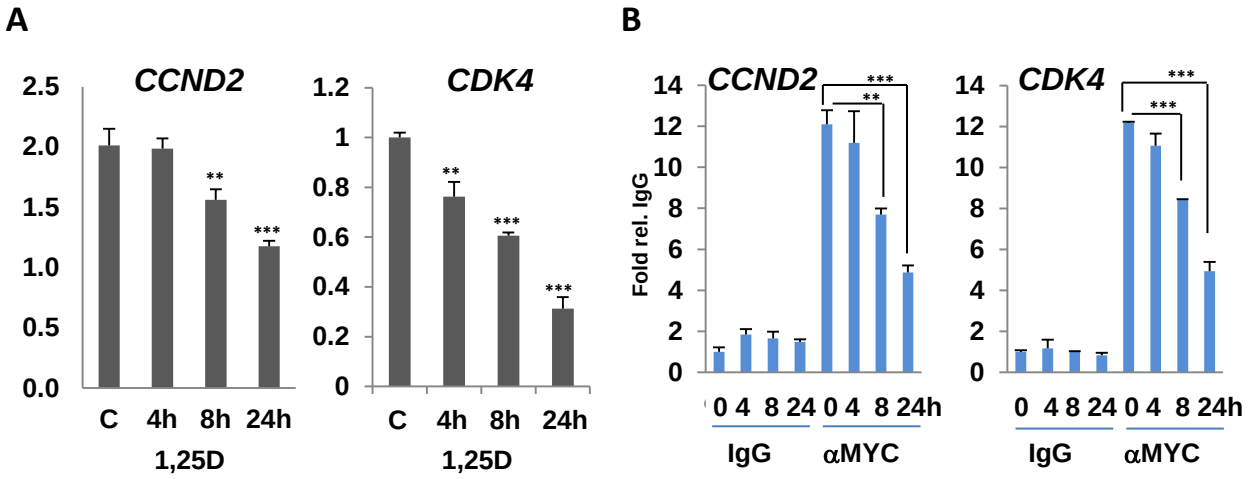

Fig. S1 A. Regulation of expression of c-MYC targets gene *CCND2* and *CDK4* in 1,25D-treated SCC25 cells. **B.** ChIP analysis of c-MYC binding to E-box regions of *CCND2* and *CDK4* in 1,25D-treated SCC25 cells. **P≤0.01, ***P≤0.001 .

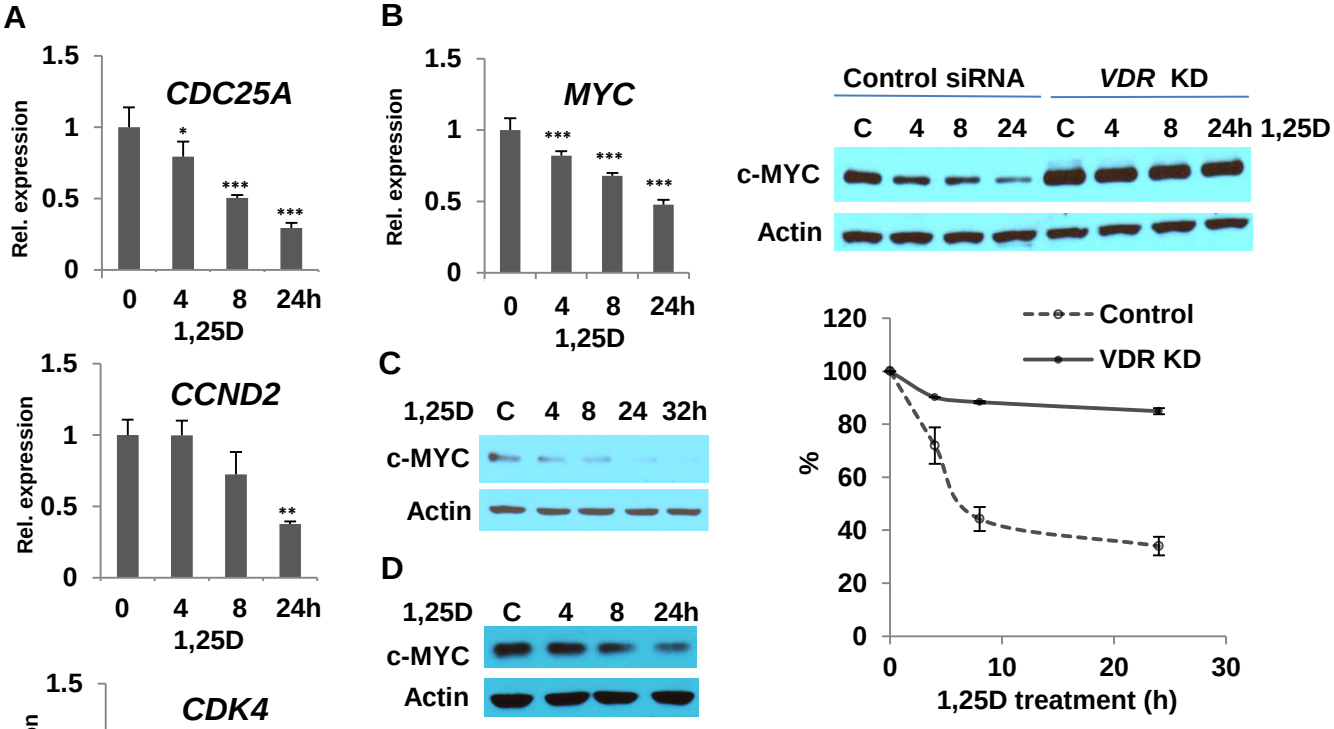

Fig. S2. A-C. Regulation of c-MYC target genes (**A**), *MYC* mRNA (**B**) and c-MYC protein (**C**) expression by 1,25D in primary human keratinocytes. **D**. Effect of 1,25D on c-MYC in HL60 promyelocytic cells. *P≤0.05, **P≤0.01, ***P≤0.001 .

Fig. S3. Effect of *VDR* knockdown on expression of c-MYC in 1,25D-treated SCC25 cells. Note elevated c-MYC expression in untreated VDR-deficient cells relative to control cells.

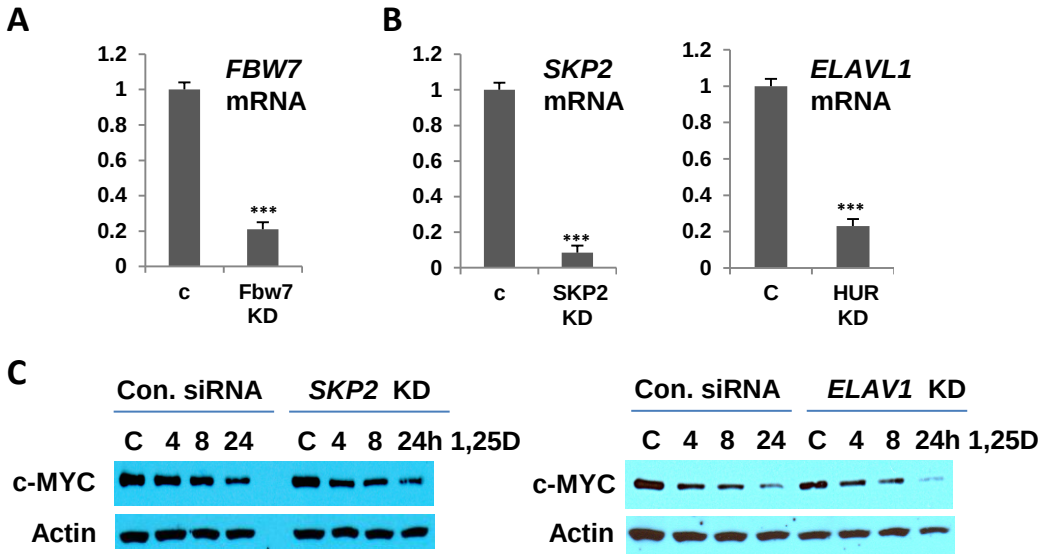

Fig. S4. A. knockdown of *FBW7* mRNA expression in SCC25 cells. **B.** Knockdown of mRNAs encoding p45SKP2 and ELAV1 (HuR) in SCC25 cells. **C.** Effects of ablation of *SKP2* or *ELAV1* on c-MYC expression in 1,25D-treated SCC25 cells. ***P≤0.001 .

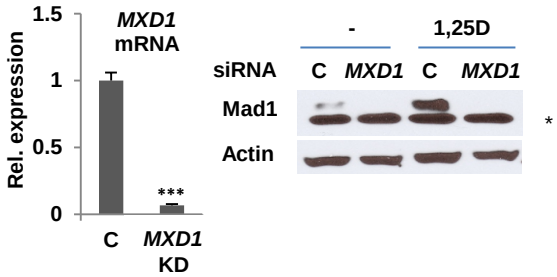

Fig. S5. Knockdown of *MXD1* mRNA (left) and protein (right) showing that the upper band observed on western blots corresponds to MXD1

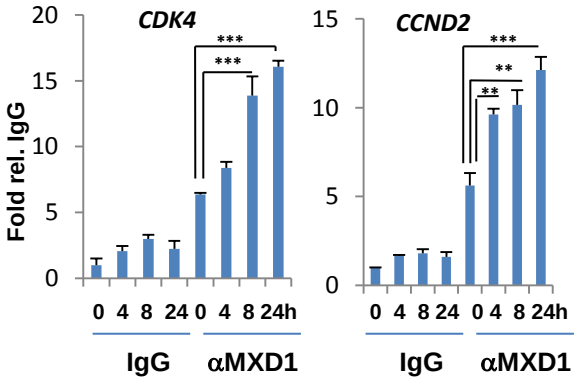

Fig. S7. ChIP analysis of MXD1 binding to E-box regions of *CCND2* and *CDK4* in 1,25D-treated SCC25 cells. **P≤0.01, ***P≤0.001.

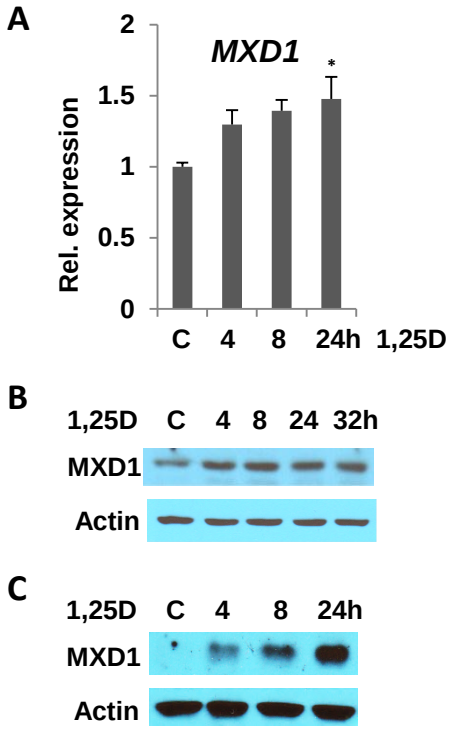

Fig. S6. Effects of 1,25D treatment on expression of *MXD1* mRNA (**A**) and protein (**B**) in primary cultures of human keratinocytes and MXD1 protein in human HL60 cells (**C**).

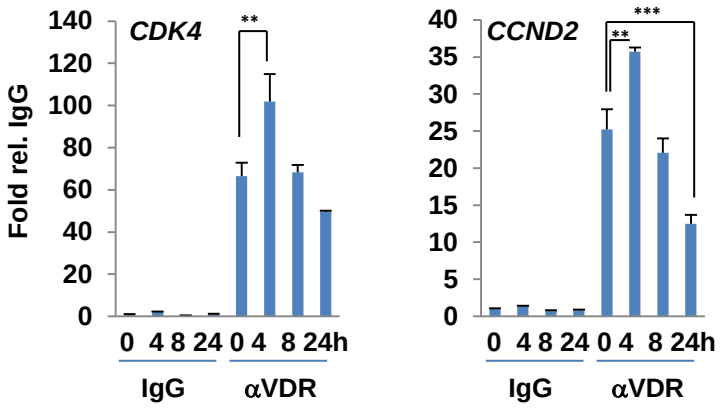

Fig. S8. ChIP analysis of association of the VDR with E-box regions of *CCND2* and *CDK4* in 1,25D-treated SCC25 cells. **P≤0.01, ***P≤0.001.

A

Parameter	Value
γ^{C}_{cMYC}	0.018 min^{-1}
γ^{V}_{cMYC}	0.026 min^{-1}
γ^{C}_{MXD1}	0.06 min^{-1}
γ^{V}_{MXD1}	0.02 min^{-1}
β^{V}_{cMYC}	0.00135 min^{-1}
β^{V}_{MXD1}	0.006 min^{-1}
α^{V}_{cMYC}	0.003 min^{-1}
α^{V}_{MXD1}	0.003 min^{-1}
λ^{C}_{cMYC}	1.8 min^{-1}
λ^{V}_{cMYC}	1.6 min^{-1}
λ^{C}_{MXD1}	6 min^{-1}
λ^{V}_{MXD1}	18 min^{-1}

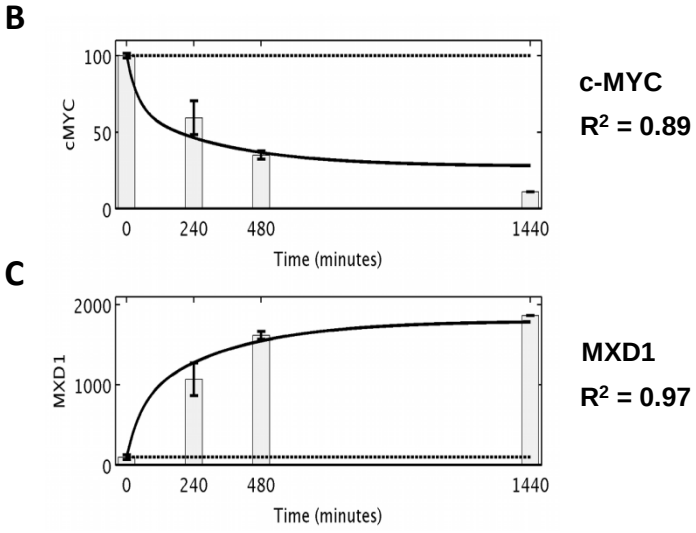

Fig. S9. A. List of parameter values derived from experiments used for mathematical modeling of c-MYC and MXD1 protein expression in B and C. See supplemental experimental procedures for details of derivations. **B.** c-MYC protein expression levels through time. The solid line represents the time-dependent solution following 1,25D addition (equation (4)). The dashed line represents the time-dependent solution under control conditions. **C.** MXD1 protein expression levels through time. The solid line represents the time-dependent solution following 1,25D application (equation (4)). The dashed line represents the time-dependent solution under control conditions.

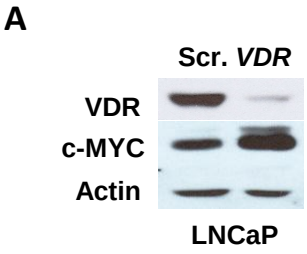

Fig. S10. Effect of ablation of the VDR on c-MYC protein expression in human LNCaP prostate carcinoma cells.

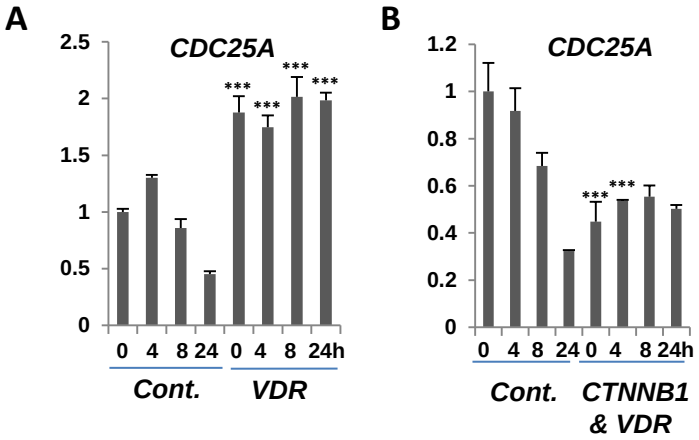

Fig. S11. Effect of knockdown of expression of the VDR alone (**A**) or in concert with β-catenin (**B**) on expression of c-MYC target gene *CDC25A* in 1,25D-treated SCC25 cells. ***P≤0.001 compared to respective control siRNA condition.

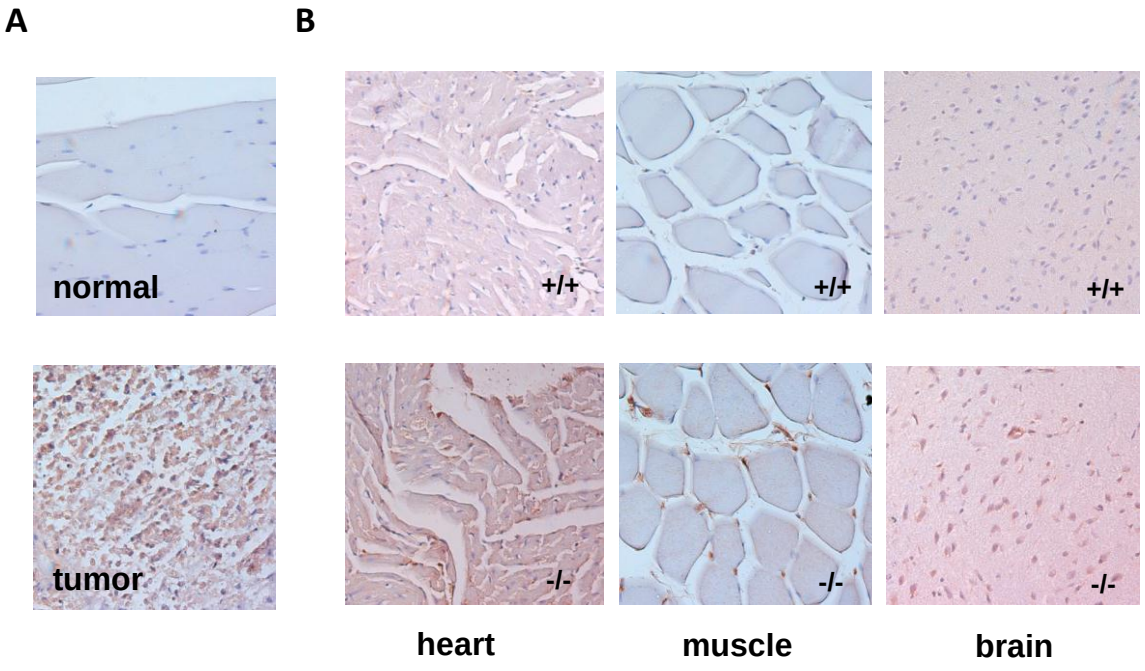

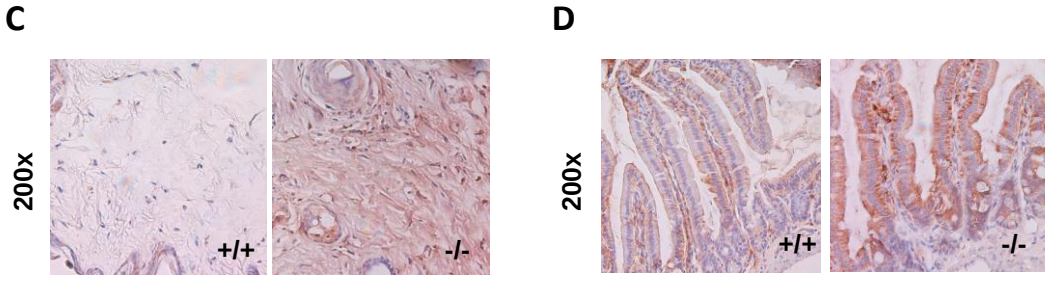

Fig. S12. A. Comparison of c-MYC expression in normal and malignant breast tissue, as a positive control for c-MYC overexpression. **B.** Immunohistochemical analysis of c-MYC expression in heart, muscle and brain of *vdr* wild-type (+/+) and knockout (-/-) mice. **C, D.** Immunohistochemical analysis of c-MYC expression in (**C**) skin and (**D**) intestine of *vdr* wild-type (+/+) and knockout (-/-) mice (200x magnification).

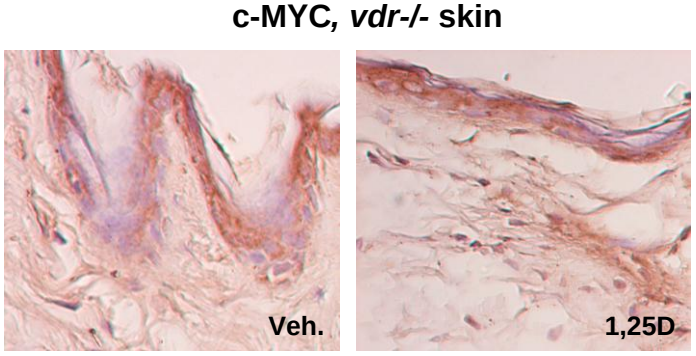

Fig. S13. 1,25D has no effect on c-MYC expression in skin of *vdr-/-* mice.

Supplemental Experimental Procedures.

Cell Culture. SCC25 cells were obtained from the American Type Culture Collection (ATCC) and cultured in DMEM/F12 (319-085-CL, Multicell) supplemented with 10% FBS. LNCaP cells were obtained from the American Type Culture Collection (ATCC) and cultured in RPMI-1640 (30-2001, ATCC) supplemented with 10% FBS. HL60 cells were obtained from ATCC and cultured in RPMI-1640-1X (350-000-CL; MULTICELL) supplemented with 10% FBS. Primary Human keratinocytes (HEK-a) were obtained from ScienCell and cultured in EpiLife® Medium (M-EPI-500-CA, Invitrogen) supplemented with Supplement S7 (S-017-5, Invitrogen).

siRNA knockdowns. SCC25 cells were transfected with siRNAs for 24 h using Lipofectamine^{TM} 2000 reagent (Invitrogen), and treated with 1,25D. siRNAs were purchased from Qiagen. The sequences of siRNAs are listed in Table 1.

RT-qPCR. Quantitative RT-PCR was performed with SsoFast-EvaGreen real-time PCR kit (Bio-Rad). Expression was normalized to the expression of *GAPDH*. Primer pairs used for RT-PCR are listed in Table 2.

Immunoprecipitation and Western blot analysis. Cells were lysed with a lysis buffer (20 mM Tris, pH 7.5, 100 Mm NaCl, 0.5% Nonidet P-40, 0.5mM EDTA, 0.5 mM phenylmethylsulfonyl fluoride). 4 μg anti-VDR (D-6; Santa Cruz) Antibody was pre-bound for 2 h to protein A agarose beads, then was washed with PBS plus 5% BSA and added to the lysate, followed by overnight immunoprecipitation. Protein A agarose beads were then washed five times with washing buffer

(20 mM Tris, pH 7.5, 200 Mm NaCl, 1% Nonidet P-40, 0.5mM EDTA, 0.5 mM phenylmethylsulfonyl fluoride) and processed for Western blotting, performed with standard protocols. The following antibodies were used: VDR (H-81), c-MYC (9E10), VDR (D-6), MXD1(c-19), all from Santa Cruz, and c-MYC (D84C12; Cell Signaling). For western blot of mouse skin, 50 mg of skin were ground under liquid nitrogen and homogenized in 1ml of lysis buffer. Lipids were removed by centrifugation at 10,000 RPM for 10min at 2^{o}C. Western blots were quantified using ImageJ 1.45 software.

ChIP assays. Cells were cross-linked with 4% paraformaldehyde for 25 min and were lysed with 500 μl lysis buffer (150 mM NaCl, 0.5% NP-40, 1% Triton X-100, 5mM EDTA and 50 mM Tris-HCl, pH 7.5) containing 1x protease inhibitor cocktail. Chromatin was sheared to an average length of 300–500 bp by sonication and supernatants were collected after centrifugation. 4 μg of Antibody was added to chromatin for immunoprecipitation overnight. then protein A agarose beads, ssDNA and BSA was added to the antibody chromatin complexes for 4 h. Protein A Agarose bead–chromatin complexes were then washed three times in TSE I (20 mM Tris-HCl, pH 8.1, 2 mM EDTA, 0.1% SDS, 1% Triton X-100 and 150 mM NaCl) followed by one wash with TSE II buffer (20 mM Tris-HCL, pH 8.1, 2 mM EDTA, 0.1% SDS, 1% Triton X-100 and 500 mM NaCl) and one wash with buffer III (0.25 M LiCl, 1% NP-40, 1% deoxychlolate, 1mM EDTA, 10mM Tris-Hcl, pH 8.1). Immunoprecipitated chromatin was then extracted with extraction buffer (1% SDS and 0.1 M NaHCO3) and was heated at 65 °C for overnight for reversal of the paraformaldehyde crosslinking. DNA fragments were purified with a PCR purification kit (Qiagen) and were analyzed by SsoFast-EvaGreen real-time PCR. The following antibodies were used for ChIP: anti-c-MYC (N-262), anti-Sin3a (K-20), anti-HDAC2 (H-54),

anti-Mad1 (c-19), and anti-VDR (D-6), all from from Santa Cruz, and anti-β−catenin (9562L) and anti-c-MYC (9402) from Cell Signaling. Primer pairs used for ChIP assays are listed in Table 3. CCND2, MYC and CDK4 primers (1) and MYC primers for β−catenin CHIP assay (2) have been described. For re-ChIP assays, VDR immunocomplexes were eluted by adding 40µl 10mM DTT for 30 min at 37°C. Supernatants were diluted 1:20 in dilution buffer (150 mM NaCl, 1% Triton X-100, 2mM EDTA and 50 mM Tris-HCl, pH 8), and re-ChIP was performed using anti-c-MYC or anti-MXD1 antibodies, as indicated in the figures.

Comparative analysis of ChIPseq data sets for the VDR and c-MYC. A *de novo* analysis of VDR ChIPseq data sets generated in the human lymphoblastoid cell line (LCL) GM10855 [GEO accession number GSM558634; (2)] were compared to a c-MYC ChIPSeq data set generated in LCL GM12878 [GEO accession number GSM754334; (3)]. Peaks in all data sets were called using model-based analysis for ChIP-Seq (MACS) (4) run using default parameters (p-value cut-off $1x10^{-5}$). The Venn diagram was generated on the data intersections using cistrome integrative analysis toolbox (5).

Mathematical Modeling of c-MYC/MXD1 expression and turnover: 1,25D application dramatically affects the c-MYC and MXD1 steady-state values, and more modestly affects the mRNA synthesis and protein degradation rates. We propose a possible mechanism underlying the change in protein levels using a quantitative analysis.

We modeled the effects of 1,25D signaling on c-MYC and MXD1 expression:

$$\frac{dx_j^i}{dt} = \beta_j^i - \alpha_j^i x_j^i \quad (1)$$

$$\frac{dy_j^i}{dt} = \lambda_j^i h(x_j^i, t) - \gamma_j^i y_j^i \quad (2)$$

where x_j^i represents an mRNA level; y_j^i represents a protein level; β_j^i is an mRNA synthesis rate; λ_j^i is a rate of production per mRNA molecule; $h(x_j^i, t)$ is the amount of circulating mRNA; and α_j^i and γ_j^i are degradation rates for mRNA and protein, respectively. The superscript i represents control conditions (C) or 1,25D treatment (V). The subscript j represents c-MYC or MXD1. We computed the time-dependent solutions by solving the system of linear differential equations:

$$x_j^i(t) = \frac{\beta_j^i}{\alpha_j^i} + \left(x_j^i(0) - \frac{\beta_j^i}{\alpha_j^i}\right)\exp(-\alpha_j^i t) \quad (3)$$

$$y_j^V(t) = y_j^V(0)\exp(-\gamma_j^V t) + \frac{\lambda_j^V \beta_j^V}{\gamma_j^V \alpha_j^V}\left(1 - \exp(-\gamma_j^V t)\right) + \left(\frac{\lambda_j^V\left(1-\frac{\beta_j^V}{\alpha_j^V}\right)}{\gamma_j^V - \alpha_j^V}\right)\left(\exp\left(-\alpha_j^V t\right) - \exp(-\gamma_j^V t)\right) \quad (4)$$

We determine the parameters in these equations using least squares fits to the data (see Fig. S9A). We use the experimentally measured levels of c-MYC mRNA (Fig. 1C) and MXD1 mRNA (Fig. 2A) to determine the parameters in Eq. (3) and the experimentally measured degradation rates of c-MYC (Fig. 1G) and MXD1 (Fig. 2C) to determine the protein decay rates in Eq. (4). These parameters can then be used to predict the time course for the protein production of c-MYC (Figs. 1E and S9B) and MXD1 (Figs. 2B and S9C) following addition of 1,25D, where we determine the values of λ_j^i based on least squares fits to the data assuming the other constants as determined from the previous experiments and normalizing to an initial value of 100. The agreement of the theoretical predictions using the parameters determined in other experiments (the R-squared value for c-MYC was 0.89 and the R-squared value for MXD1 was

0.97 see Fig. S9) provides strong evidence for the validity of the model and the reliability of the experimental data.

Animal Experiments. All animal experiments were carried out in compliance with and approval by the Institutional Animal Care and Use Committee. *vdr*+/- animals (The Jackson Laboratory, Bar harbor, ME) were mated to generate homozygous for $vdr^{-/-}$ mice. At 21 days of age, control $vdr^{+/+}$ and $vdr^{-/-}$ mice were weaned and maintained until sacrifice on high calcium diets containing 1.5% calcium in the drinking water and autoclaved regular chow.

Genotyping of Mice. Genomic DNA was isolated from tail fragments by standard phenol/chloroform extraction and isopropyl alcohol precipitation. To determine the genotype at VDR loci, 2 PCRs were conducted for each animal. The wild type VDR allele was detected using forward primer 5′-CTGCCCTGCTCCACAGTCCTT-3′ and reverse primer 5′-CGAGACTCTCCAATGTGAAGC-3′. The disrupted VDR allele was assayed using the neo forward primer 5′-GCTGCTCTGATGCCGCCGTGTTC-3′ and a neo reverse primer 5′-GCACTTCGCCCAATAGCAGCCAG-3′. PCR conditions were 30 cycles for all VDR and disrupted VDR allele, 94 °C for 1 min, 65 °C for 1 min, and 72 °C for 1 min; and neomycin, 94 °C for 1 min, 60 °C for 1 min, and 72 °C for 1 min.

Topical treatment with 1,25D. Mice (5-6) at 3 months of age were treated topically on the dorsal surface with vehicle or 1,25D for 18 h. The vehicle was a base lotion containing ethanol: propylene-glycol: water (2:1:1). The 1,25D (Sigma) was dissolved in ethanol and diluted with vehicle. Each mouse was treated with vehicle (100μl/cm^2) on the highest part of the back (neck)

and with 1,25D (15ng/100µl/cm^2) on the lowest part of the back (hip) to avoid the contact between 2 treatments. After 18 h of treatment the treated region of skin were immediately removed and fixed in PLP fixative (2% paraformaldehyde containing 0.075 M lysine and 0.01 M sodium periodate) overnight at 4 °C, washed and processed immunohistochemistry (IHC) study.

Immunohistochemistry. c-MYC, Setd8, and MXD1 expression were determined by IHC using the avidin-biotin-peroxidase complex (ABC) technique. Anti-c-MYC (9E10; Santa Cruz), anti-SET8 (C18B7; Cell Signalling), or anti-MXD1 (SAB2105310; Sigma-Aldrich) were applied to dewaxed paraffin sections overnight. After washing with high salt buffer, slides were incubated with secondary antibody, washed and processed using the Vectastain ABC-AP kit (Vector Laboratories) and mounted with Permount (Fisher Scientific). Images from sections were processed using Bioquant image analysis software.

Statistical Analysis. All experiments are representative of 3-5 biological replicates. Unless otherwise indicated in the figures, statistical analysis was conducted using the program SYSTAT13 by performing one-way analysis of variance (ANOVA) followed by the Tukey test for multiple comparisons as indicated: *$P \leq 0.05$, **$P \leq 0.01$, ***$P \leq 0.001$.

Table 1: siRNAs

Name of gene	siRNA Sequence
VDR	5’-TCAGACTCCATTTGTATTATA-3’
FBXW7	5’-CCCTAAAGAGTTGGCACTCTA-3’
MYC	5’-CTCGGTGCAGCCGTATTTCTA-3’
β–catenin	5’-CTCGGGATGTTCACAACCGAA-3’
MXD1	5’-CAGTAGCAGATCAACTCACAA-3’
SKP2	5’-AAGTGATAGTGTCATGCTAAA-3’
ELAVL1	5’-AAGTAGCAGGACACAGCTTGG-3’
Control	5’-CAGGGTATCGACGATTACAAA-3’

Table 2: qPCR primers

Primer Name	Sequence
CCND2-FORWARD	5’-GAGAAGCTGTCTCTGATCCGCA-3’
CCND2-REVERSE	5’-CTTCCAGTTGCGATCATCGACG-3’
CDK4-FORWARD	5’-CCATCAGCACAGTTCGTGAGGT-3’
CDK4-REVERSE	5’-TCAGTTCGGGATGTGGCACAGA-3’
CDC25A-FORWARD	5’-TCTGGACAGCTCCTCTCGTCAT-3’
CDC25A-REVERSE	5’-ACTTCCAGGTGGAGACTCCTCT-3’
MYC-FORWARD	5’-CCTGGTGCTCCATGAGGAGAC-3’
MYC-REVERSE	5’-CAGACTCTGACCTTTTGCCAGG-3’
MXD1-FORWARD	5’-ACCTGAAGAGGCAGCTGGAGAA-3’
MXD1-REVERSE	5’-AGATAGTCCGTGCTCTCCACGT-3’
ELAVL-1-FORWARD	5’-CCGTCACCAATGTGAAAGTG-3’
ELAVL-1-REVERSE	5’-TCGCGGCTTCTTCATAGTTT-3’
SKP2-FORWARD	5’-CTCCACGGCATACTGTCTCA-3’
SKP2-REVERSE	5’-GGGCAAATTCAGAGAATCCA-3’
FBW7-FORWARD	5’-CAGCAGTCACAGGCAAATGT-3’
FBW7-REVERSE	5’-GCATCTCGAGAACCGCTAAC-3’
CTNNB1-Forward	5’-CACAAGCAGAGTGCTGAAGGTG-3’
CTNNB1-Reverse	5’-GATTCCTGAGAGTCCAAAGACAG-3’

Table 3: Primers for ChIP assays.

Primer Name	Sequences
CDC25A-FORWARD	5'-GAGAGATCAGGCCAGGAAAC-3'
CDC25A-REVERSE	5'-CTCTCCCGCCCAACATTC-3'
CDK4-FORWARD	5'-GAGCGACCCTTCCATAACCA-3'
CDK4-REVERSE	5'-GGGCTGGCGTGAGGTAAGT-3'
MYC-FORWARD	5'-TGGGCGGCTGGATACCTT-3'
MYC-REVERSE	5'-GATGGGAGGAAACGCTAAAGC-3'
CCND2-FORWARD	5'-TCAGTAAATGGCCACACATGTG-3'
CCND2-REVERSE	5'-GGAGCTCTCGACGTGGTCAA-3'
MYC-FORWARD	5'-AGGCAACCTCCCTCTCGCCCTA-3'
MYC-REVERSE	5'- AGCAGCAGATACCGCCCCTCCT-3'

References

1. Zeller KI, *et al.* (2006) Global mapping of c-Myc binding sites and target gene networks in human B cells. *Proceedings of the National Academy of Sciences of the United States of America* 103(47):17834-17839.
2. Ramagopalan SV, *et al.* (2010) A ChIP-seq defined genome-wide map of vitamin D receptor binding: Associations with disease and evolution. *Genome Research* 20(10):1352-1360.
3. Rozowsky J, *et al.* (2011) AlleleSeq: analysis of allele-specific expression and binding in a network framework. *Mol. Syst. Biol.* 7.
4. Zhang Y, *et al.* (2008) Model-based Analysis of ChIP-Seq (MACS). *Genome Biology* 9(9).
5. Liu T, *et al.* (2011) Cistrome: an integrative platform for transcriptional regulation studies. *Genome Biology* 12(8).